Electrochemistry and Electrogenerated Chemiluminescence of Three Phenanthrene Derivatives, Enhancement of Radical Stability, and Electrogenerated Chemiluminescence Efficiency by Substituent Groups

Honglan Qi,[†] Yu-Han Chen,[‡] Chien-Hong Cheng,[‡] and Allen J. Bard*,[†]

[†]Center for Electrochemistry, Department of Chemistry and Biochemistry, The University of Texas, Austin, Texas 78712, United States

[‡]Department of Chemistry, National Tsing-Hua University, Hsinchu 30013, Taiwan

Ⓢ *Supporting Information*

ABSTRACT: The electrochemistry and electrogenerated chemiluminescence (ECL) of three phenanthrene derivatives, 3,6-diphenyl-9,10-bis-(4-*tert*-butyl-phenyl)phenanthrene (TphP, T1), 3,6-di(naphthalen-2-yl)-9,10-bis(4-*tert*-butylphenyl)phenanthrene (TnaP, T2), and 3,6-di(pyren-1-yl)-9,10-bis(4-*tert*-butylphenyl)phenanthrene (TpyP, T3), are investigated in an acetonitrile:benzene (v:v = 1:1) solvent. Cyclic voltammetry (CV) of the three derivatives shows reversible reduction waves and less chemically reversible oxidation waves at low scan rates. The CV character becomes more reversible, and the stability of the radical cations increases as the conjugation of the substituent groups appended to the phenanthrene increases. This finding indicates that the radical ion stabilities in phenanthrene derivatives are drastically improved by increasing the conjugation of the substituent groups; thus, electrochemically stable radical ions can be obtained by introducing more conjugated groups to the phenanthrene center. Additionally, ECL is generated for all compounds by radical ion annihilation, and the ECL spectrum shows good agreement with the fluorescence emission, assigned as emission by the S-route. ECL efficiencies for radical ion annihilation are 0.004 for TphP, 0.16 for TnaP, and 0.25 for TpyP, respectively, and the ECL efficiency increases with the conjugation of the substituent groups appended to the phenanthrene increases. Radical ion annihilation produced by potential steps exhibits asymmetric ECL transients in which the cathodic ECL pulse is smaller than the anodic pulse due to the instability of the radical cation. These molecules can produce a stronger ECL, which can be observed by the naked eye in a lighted room, on reduction in the presence of a coreactant (benzoyl peroxide).
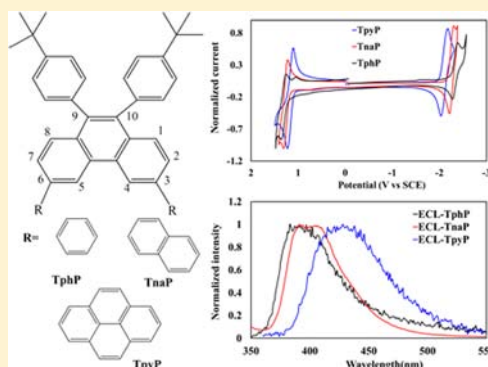
INTRODUCTION

We report here the electrochemistry and electrogenerated chemiluminescence (ECL) of three 9,10-bis(4-*tert*-butyl-phenyl)phenanthrene derivatives (as shown in Scheme 1), 3,6-diphenyl-9,10-bis-(4-*tert*-butylphenyl)phenanthrene (TphP, T1), 3,6-di(naphthalen-2-yl)-9,10-bis(4-*tert*-butylphenyl)-phenanthrene (TnaP, T2), and 3,6-di(pyren-1-yl)-9,10-bis(4-*tert*-butylphenyl)phenanthrene (TpyP, T3). They all have high external quantum efficiency and have been studied as a blue-emitting electroluminescent species for organic light-emitting diodes (OLEDs).[1]

ECL is a chemical phenomenon in which light emission is produced by an energetic electron-transfer reaction between electrochemically generated species at an electrode surface. The various mechanisms of ECL processes have been discussed extensively.[2] As shown here and in previous publications, there are two general methods to produce ECL. The first is radical ion annihilation, in which radical ions of an organic compound (A) are generated sequentially at the surface of an electrode by

cycling the potential within a short time interval and react (annihilate) during their interdiffusion. The annihilation by ECL between radical cations and anions produces an excited state (A*) if the energy provided by the electron-transfer reaction is sufficient. When A* is in the singlet state, the compound reacts via what is called the S-route or an "energy-sufficient system" (eqs 1−4).
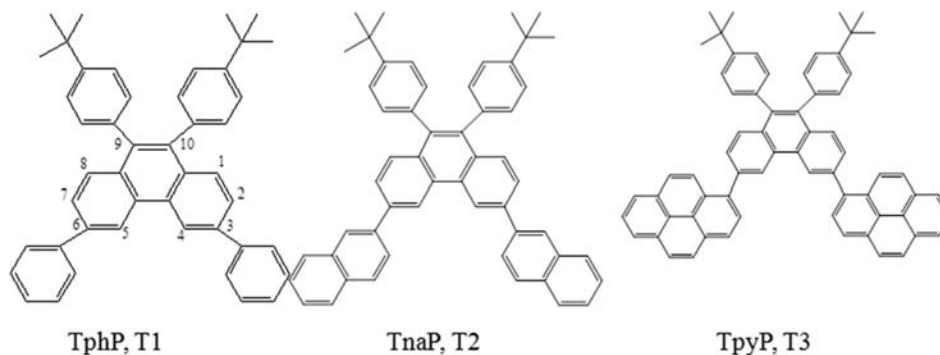
$$A + e^- \rightarrow A^{-\bullet} \quad (1)$$

$$A - e^- \rightarrow A^{+\bullet} \quad (2)$$

$$A^{-\bullet} + A^{+\bullet} \rightarrow {}^1A^* + A \quad (3)$$

$${}^1A^* \rightarrow A + h\nu \quad (4)$$

If the energy provided by the ion radicals is not sufficient to populate the singlet state, the triplet state can be populated (eq
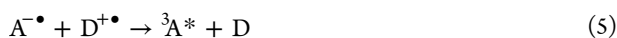
Scheme 1. Structure of the Phenanthrene Derivatives

TphP, T1   TnaP, T2   TpyP, T3

5), followed by a triplet−triplet annihilation to generate the singlet state (eq 6). This mechanism is called the T-route or an "energy-deficient system".

$$A^{-\bullet} + D^{+\bullet} \rightarrow {}^3A^* + D \tag{5}$$

$$^3A^* + {}^3A^* \rightarrow {}^1A^* + A \tag{6}$$

In these situations, light emission is highly dependent upon the stability of these radical ions; therefore, any side reactions that involve either radical ion can decrease the number of electron transfer reactions and, in turn, the emission intensity. If either the cation radical or the anion radical is unstable, or these radical ions cannot be generated prior to the oxidation or reduction of solvent or supporting electrolyte, ECL can often be generated by use of a coreactant, which produces either a strong reducing agent when oxidized (such as oxalate or tripropylamine) or a strong oxidizing agent when reduced (such as peroxydisulfate or benzoyl peroxide (BPO)). For example, the mechanism of the BPO-based system can be presented as

$$BPO + e^- \rightarrow BPO^{-\bullet} \tag{7}$$

$$BPO^{-\bullet} \rightarrow C_6H_5CO_2^- + C_6H_5CO_2^{\bullet} \tag{8}$$

$$C_6H_5CO_2^{\bullet} + A^{-\bullet} \rightarrow C_6H_5CO_2^- + {}^1A^* \tag{9}$$
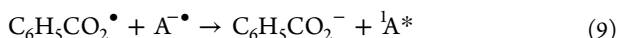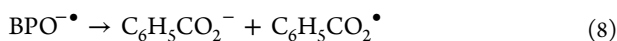
The coreactant can often be used to help elucidate the ECL reaction mechanisms by comparing the ECL behavior with the regular annihilation ECL.

We have previously reported the electrochemical and ECL behavior of several aromatic compounds, such as fluorene,[3−9] anthracene,[10−16] BODIPY,[17−22] perylene,[23] pyrenophanes,[24] silole,[25] and phenothiazine.[26,27] The core structure and substituent groups strongly affected the electrochemistry and ECL behavior. Even with strong photoluminescence, however, some molecules do not produce strong ECL because the decomposition of the radical ions causes one of the redox processes to be chemically irreversible. Thus, increasing the radical stability for efficient ECL materials is crucial for the development of new high-performance light-emitting materials. Most studies of the ECL behavior of organic compounds have sought to change the absorption and emission maxima by altering their photophysical properties through intramolecular charge transfer[28] or have only attempted to characterize the ECL properties of new ECL-active materials.[4] Only a few examples of the enhancement of ECL efficiency by systematically improving the radical stability of organic compounds have been reported.[29,30] Our interests are focused on investigating the electrochemical and ECL behavior of organic compounds

as a function of structure and finding novel compounds that generate ECL efficiently without the addition of a coreactant or additional compound.

As previous reports have demonstrated, the anthracene moiety is the most common core structure for blue fluorescent materials in OLEDs, and the ECL of anthracene derivatives has been reported.[10−16] As an isomer of anthracene, phenanthrene is one of the most versatile fused aromatic compounds. Phenanthrene has higher resonance energy and is therefore more stable,[31] and it has been used as the core structure in OLEDs because of its efficient blue-light emission and good chemical and thermal stabilities. However, only a few blue fluorescent materials using phenanthrene as the core structure have been identified to date, such as tetraalkoxyphenanthrene,[32] diiodophenanthrenes,[33] oligomeric phenanthrene,[34−36] and polyphenanthrene.[37,38] Although phenanthrene is a good emitting center, it has poor cation radical stability. By functionalization with the appropriate substituent groups, it is possible to improve the stability of the oxidized phenanthrene for ECL. Recently, the synthesis and photo- and electro-luminescent properties of 3,6-disubstituted phenanthrenes have been reported for their use as an alternative host material with blue fluorophores. These compounds exhibit excellent photo-luminescent and thermal properties for electroluminescent applications.[1]

Here, we report the electrochemistry and ECL behavior of three phenanthrene derivatives in solution. We correlate their electrochemical properties and ECL behavior with their specific structures. The structures of the three phenanthrene derivatives with different substituent groups are shown in Scheme 1. These phenanthrene derivatives contain a phenanthrene core with two 4-*tert*-butylphenyl groups at the C-9 and C-10 positions and two different substituents, different combinations of phenyl (TphP, T1), naphthyl (TnaP, T2), and pyrenyl (TpyP, T3), in the C-3 and C-6 positions. The photophysical and electro-chemical properties of these compounds have already been investigated.[1] Here, we would like to provide a broader and systematic overview of the electrochemical and ECL properties of the phenanthrene derivatives in acetonitrile and benzene mixed solvent to generate information to guide the synthesis of new phenanthrene compounds.

■ EXPERIMENTAL SECTION

Materials. Anhydrous (MeCN, 99.8%) and anhydrous benzene (Bz, 99.8%) were obtained from Sigma-Aldrich (St. Louis, MO) and transferred directly into an argon-atmosphere glovebox (MBraun Inc., Stratham, NH) without further purification. Electrochemical-grade tetra-*n*-butylammonium hexafluorophosphate (TBAPF$_6$) was dried in a vacuum oven at 100 °C and then transferred directly into an argon-

atmosphere glovebox. Benzoyl peroxide (BPO) was purchased from Sigma-Aldrich and used as received. The synthesis of 3,6-diphenyl-9,10-bis-(4-*tert*-butylphenyl)phenanthrene (TphP, T1), 3,6-di-(naphthalen-2-yl)-9,10-bis(4-*tert*-butylphenyl)phenanthrene (TnaP, T2), and 3,6-di(pyrene-1-yl)-9,10-bis(4-*tert*-butylphenyl)-phenanthrene (TpyP, T3) has been described previously.[1]

Apparatus and Methods. UV−vis spectra were recorded using a 1 cm quartz cuvette on a Milton Roy Spectronic 3000 array spectrophotometer. Fluorescence spectra were recorded by using a Fluorolog-3 (Horiba Scientific, Inc., France). UV−vis absorbance and fluorescence measurements were carried out in MeCN:Bz (v:v = 1:1) solvent under air-saturated conditions.

MeCN:Bz (v:v = 1:1) was used as the solvent and 0.1 M $TBAPF_6$ as the supporting electrolyte for all electrochemical investigations. All electrochemical experiments were performed under anhydrous conditions. For measurements made outside of the glovebox, the electrochemical cell was assembled inside the glovebox and sealed with a Teflon cap with a rubber O-ring. Stainless steel rods driven through the cap formed the electrode connections. Electrochemical experiments were performed using a three-electrode setup with a Pt disk working electrode, a Pt auxiliary electrode, and a silver wire quasi-reference electrode. A Pt disk sealed in glass was bent at a 90° angle so that the electrode surface could face the light detector. The area of the Pt disk electrode was 0.043 cm^2. The working electrode was polished after each experiment with 0.3 μm alumina (Buehler, Ltd., Lake Bluff, IL) for several minutes, sonicated in water and in ethanol for 5 min each, and dried in an oven at 120 °C. Cyclic voltammetry (CV) potentials were calibrated with ferrocene as a standard, taking E^0 = 0.342 V vs SCE.[39] CV and chronoamperometry measurements were carried out with a CHI 660 electrochemical workstation (CH Instruments, Austin, TX). DigiSim 3.03 software (Bioanalytical Systems, Inc., West Lafayette, IN) was used to simulate the cyclic voltammograms.

The ECL transients and simultaneous CV and ECL measurements were recorded using an Autolab electrochemical workstation (NOVA 1.7, Metrohm Inc.) coupled with a photomultiplier tube (PMT, Hamamatsu R4220p, Japan) held at −750 V with a high-voltage power supply (Kepco, Flushing, NY). The photocurrent produced at the PMT was transformed into a voltage signal by an electrometer/high-resistance system (Keithley, Cleveland, OH) and fed into the external input channel of an analog-to-digital converter (ADC) of the Autolab. ECL spectra were generated using CHI 660 and collected with the Fluolog 3.

■ RESULTS AND DISCUSSION

Electrochemistry. All electrochemical measurements were carried out in MeCN:Bz (v:v = 1:1) solvent with 0.1 M $TBAPF_6$ as the supporting electrolyte. The results are summarized in Table 1. Although electrochemical studies of T1−T3 had been performed previously with oxidation in CH_2Cl_2 and reduction in tetrahydrofuran,[1] these solvents are inappropriate for ECL because of their rather narrow potential windows.[16] Figure 1 shows the cyclic voltammograms (CVs) of

Table 1. Summary of Electrochemical Data in MeCN:Bz (v:v = 1:1)

	$E_{1/2}$ (V vs SCE)[a]		$10^6 D$	$-\Delta G_{ann}$	$-\Delta H_{ann}$	E_g
	A/A^{+a}	A/A^{-a}	(cm^2 s^{-1})	(eV)[b]	(eV)[b]	(eV)[c]
TphP	+1.33	−2.33	6.69	3.66	3.56	3.66
TnaP	+1.28	−2.24	5.9	3.52	3.42	3.52
TpyP	+1.16	−2.10	4.74	3.26	3.16	3.26

[a]$E_{1/2}$ values are obtained either by averaging the cathodic and anodic peak potentials or by digital simulation. [b]$-\Delta G_{ann} = E_{pa,ox} - E_{pc,red}$, $-\Delta H_{ann} = -\Delta G_{ann} - 0.1$. [c]$E_g = E_{pa,ox} - E_{pc,red}$.
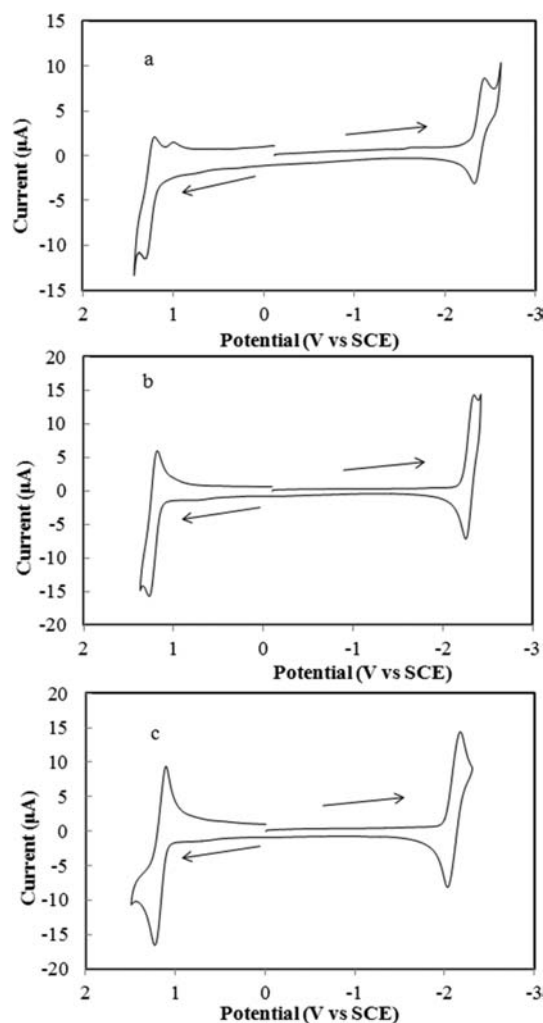

Figure 1. Cyclic voltammograms of (a) 0.5 mM TphP, (b) 0.5 mM TnaP, and (c) 0.8 mM TpyP in MeCN:Bz (v:v = 1:1) solvent containing 0.1 M $TBAPF_6$. Scan rate: 0.5 V/s. Pt electrode area: 0.043 cm^2. All scans start in the negative direction.

TphP (a), TnaP (b), and TpyP (c) at the Pt electrode in MeCN:Bz−0.1 M $TBAPF_6$ with a scan rate of 0.5 V/s. The CV of TphP at a scan rate of 0.5 V/s showed a less reversible one-electron oxidation with a half-wave potential $E_{1/2}$ = +1.33 V vs SCE. The reverse wave is much smaller than its oxidation, and a new reduction wave of a product appears on the reverse scan at 1.0 V. This observation indicates that the radical cation formed at ∼1.33 V is unstable and a chemical reaction follows right after the radical cation is produced. It could have formed a dimer through the coupling of the two phenyl units at the C3 or C6 position.[40] At higher scan rates, for example, 10 V/s, the reduction wave at 1.0 V disappeared, and the oxidation wave became more reversible (as shown in Supporting Information, Figure S1a). The negative scan showed a nernstian reduction wave at $E_{1/2}$ = −2.33 V vs SCE. The observed peak separation (ΔE_p) of ∼112 mV is larger than the expected value for a one electron transfer nernstian behavior, 57 mV. This can be attributed to the high uncompensated resistance ($R_u \approx 1600$ Ω), which is frequently observed with aprotic solvents. When the phenanthrene core is blocked with a naphthyl group at 3 and 6 positions (TnaP), the oxidation of TnaP is easier and more chemically reversible at $E_{1/2}$ = 1.28 V vs SCE, even at ν = 1 V/s (as shown in Supporting Information, Figure S1b). This
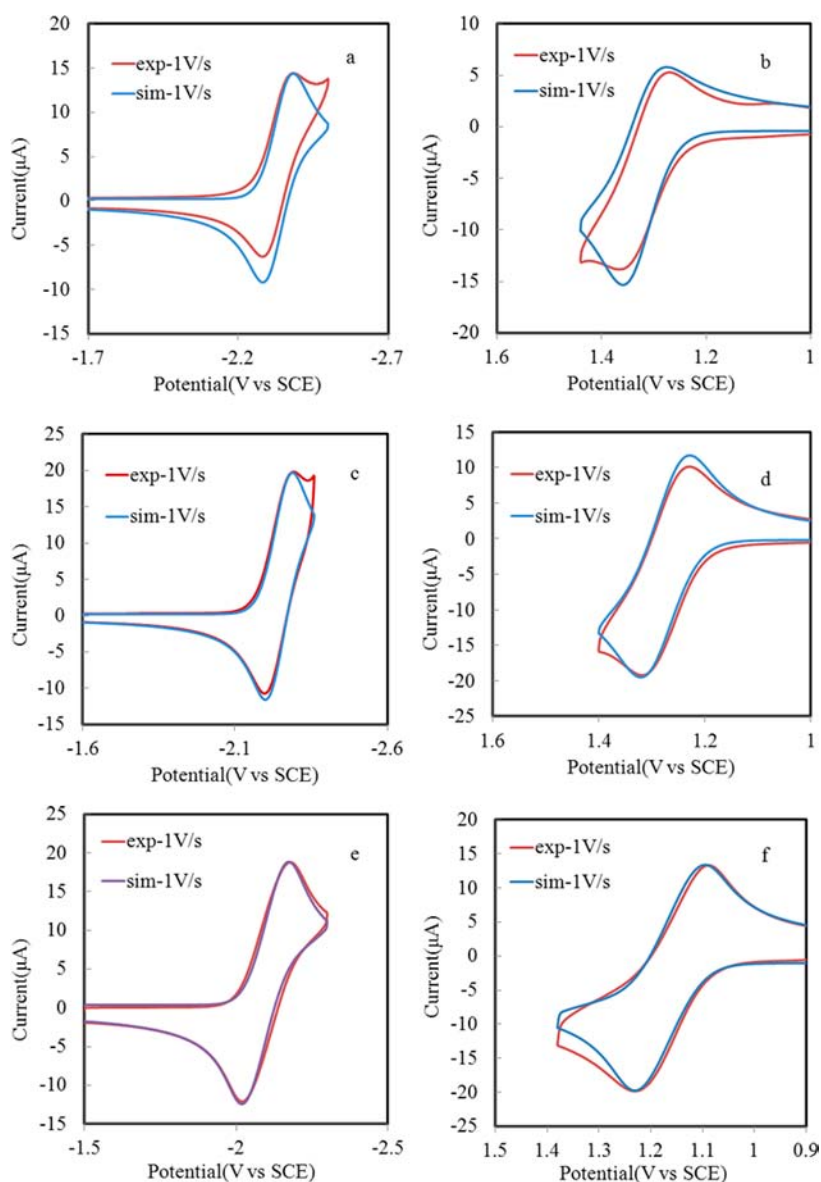
Figure 2. Comparison between simulated and experimental oxidation and reduction waves for T1−T3 at 1 V/s. Simulation model: (a) reduction of 0.5 mM TphP (E, k^0 = 0.025 cm/s); (d) oxidation of 0.5 mM TphP (EC, k^0 = 10 000 cm/s, k_{eq} = 1, k_f = 10 s); (c) reduction of 0.5 mM TnaP (E, k^0 = 0.2 cm/s); (b) oxidation of 0.5 mM TnaP (E, k^0 = 0.1 cm/s), (e) reduction of 0.8 mM TpyP (E, k^0 = 0.05 cm/s); and (f) oxidation of 0.8 mM TpyP (E, k^0 = 0.2 cm/s).

result indicates that the anodic radical ion of TnaP is more stable than that of TphP. The negative scan showed a reversible reduction wave at $E_{1/2}$ = −2.24 V vs SCE for TnaP. For TpyP, the most highly blocked compound at the 3 and 6 positions due to the presence of the pyrene group showed chemically reversible, nernstian oxidation and reduction waves at $E_{1/2}$ = +1.16 V and $E_{1/2}$ = −2.10 V vs SCE, respectively, even at ν = 0.5 V/s, indicating the stability of the radical ions on the time scale of the experiment. These electrochemical results are in good agreement with previous results in CH_2Cl_2 (oxidation) and tetrahydrofuran (reduction).[1] For these three compounds, there was a positive shift in $E_{pc,red}$ (from −2.33 to −2.10 V vs SCE) and a negative shift in $E_{pa,ox}$ (from +1.33 to +1.16 V vs SCE) with an increase in the conjugation of the molecules. As compared to the other two compounds, TpyP is more easily oxidized and reduced.

CVs obtained at different scan rates showed that the peak currents of the reduction and oxidation wave changed linearly with the square root of the scan rate ($\nu^{1/2}$, as shown in Supporting Information, Figure S2) for both the reduction ($i_{p,r}$) and the oxidation ($i_{p,o}$), indicating diffusion control for both reactions. The diffusion coefficient, D, values were determined from the Randles−Sevcik equation by plotting the peak current versus $\nu^{1/2}$ and were listed in Table 1, assuming each wave was a single electron-transfer step. Chronoamperometry at an ultramicroelectrode (UME) was also carried out to determine the number of electrons (n) and the diffusion coefficient.[41] The number of electrons obtained using the UME was found to be 1, which confirmed our assumption for the CV calculations. The D value found from the UME current transient also agreed with that from the CV method (as shown in Supporting Information, Figure S3). Before the chronoamperometry study, the linear scan voltammetry of TphP, TnaP, and TpyP at a Pt
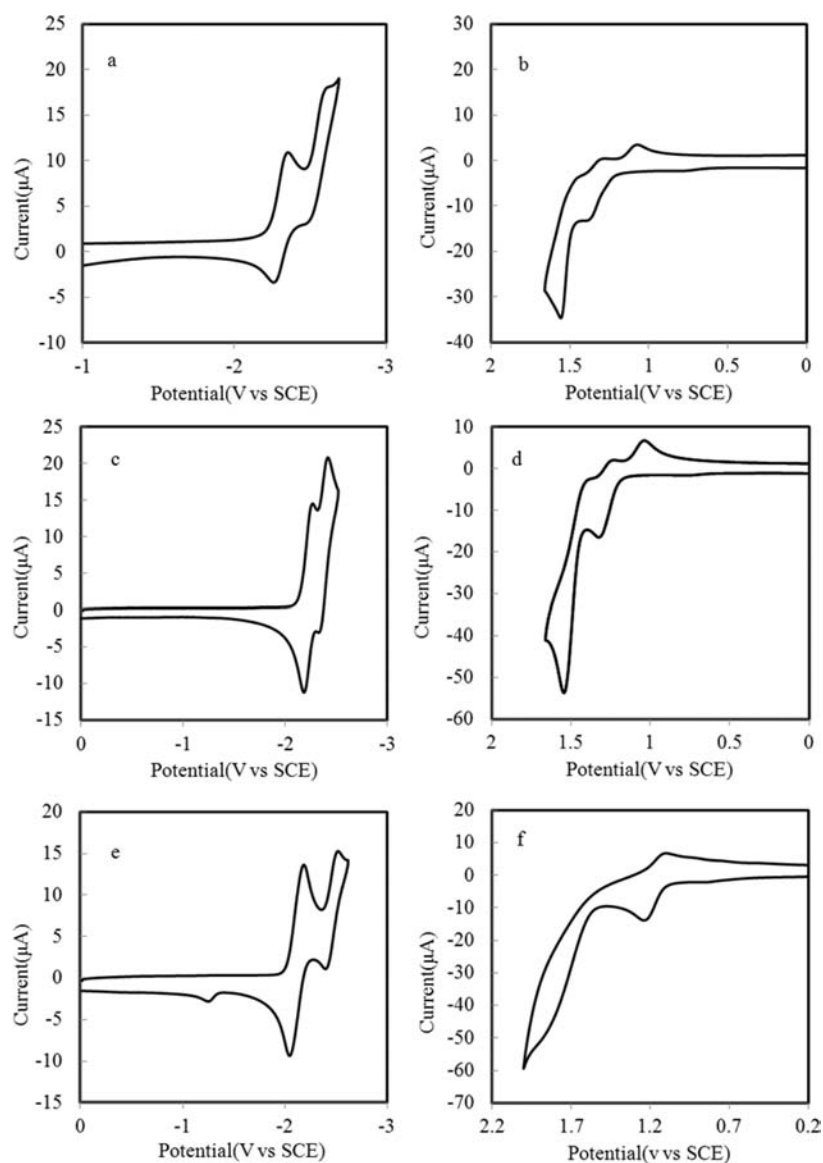
9044

dx.doi.org/10.1021/ja403166s | J. Am. Chem. Soc. 2013, 135, 9041−9049

Figure 3. Cyclic voltammograms of 0.5 mM TphP (a,b), 0.5 mM TnaP (c,d), and 0.8 mM TpyP (e,f) in MeCN:Bz (v:v = 1:1) solvent containing 0.1 M TBAPF$_6$ with a scan rate of 0.5 V/s. (a,c,e) Cathodic scans; (b,d,f) anodic scans.

UME was studied. One well-separated reduction peak and oxidation peak were observed, consistent with the CV results at the macroelectrode (as shown in Supporting Information, Figure S4).

The cyclic voltammogram were digitally simulated at different scan rates and compared to the experimental results to gain better insight into the mechanisms and rates of both the anodic and the cathodic reactions (see Figure 2 and Supporting Information, Figures S5−S10). The uncompensated resistance and capacitance were obtained by performing a potential step at potentials where no faradaic reactions occur (0.2 V vs SCE). The geometric electrode surface area used in simulations was determined by a potential step experiment performed in a solution of ferrocene in acetonitrile ($D = 1.2 \times 10^{-5}$ cm^2/s). Although both the anodic and the cathodic wave are single-electron transfer reactions, the nature of the waves is greatly affected by substituent groups. The cathodic wave of TphP is characterized by a reversible electron transfer, with a heterogeneous rate constant, k°, of approximately 0.025 cm/s (Figure 2a and Supporting Information, Figure S5). However,

the oxidation waves for TphP could be fit to an EC mechanism, a chemical reaction following an electrochemical electron transfer, with a homogeneous forward rate constant $k_f = 10$ s^{-1}, $k_{eq} = 1.0$, and a heterogeneous rate constant $k^0 = 10\,000$ cm/s. Some information about the nature of the following homogeneous chemical reactions was obtained from CVs at different scan rates (as observed in Supporting Information, Figure S6). At lower scan rates (below 1 V/s), a small reduction peak was observed at 1.0 V. This small peak disappeared at higher scan rates. These findings confirm a less reversible one-electron oxidation for TphP.

Both the cathodic and the anodic waves of TnaP were characterized by a reversible one-electron transfer with a heterogeneous rate constant, k^0, of approximately 0.2 cm/s for reduction and 0.1 cm/s for oxidation (Figure 2c,d and Supporting Information, Figures S7,S8). CV simulations using $k^0 = 0.1$ cm/s and $k^0 = 0.025$ cm/s for TpyP are in good agreement with the experimental data at scan rates (ν) from 0.02 to 5 V/s, also indicating a reversible one-electron transfer for the cathodic and anodic CVs of TpyP (Figure 2e, f and

Supporting Information, Figures S9,S10). The best fit between the experimental and simulated CVs for Tnap and TpyP was observed from 0.02 to 5 V/s, assuming that the reduction and oxidation mechanism is a simple electron transfer with no coupled homogeneous chemical reactions. This relatively slow electron transfer for a simple outer-sphere reaction might be caused by a large conformational change in the molecule upon reduction or oxidation.

In summary, first, the CV character becomes more reversible and the stability of the radical cation increases as the conjugation of the substituent groups appended to the phenanthrene increases. The enhanced radical stability of the three compounds after reduction or oxidation is due to strong electron conjugation in these compounds, which is confirmed by the photophysical results shown in the following section. Second, as previously reported,[1] the electrochemical HOMO−LUMO (highest occupied molecular orbital, HOMO; lowest unoccupied molecular orbital, LUMO) gradually decreases as the conjugation of the substituent groups increases, which is in good agreement with the energy-gap trends obtained from the lowest UV−vis absorption values and the maxima of the emission and ECL spectra. This result suggests that, among the three compounds, more effective conjugation occurs by increasing the conjugation of the substituent groups. Thus, the electrochemically stable radical can be obtained by merely introducing more conjugated groups to the phenanthrene center.

Oxidation and reduction scans of three compounds to more negative and more positive potentials can provide information about the energies needed to form the dianions and dications of these compounds. The reduction and oxidation of the three compounds at more negative and more positive potentials generally produced a second peak attributed to the addition of a second electron (Figure 3). The separation between the first and second waves (ΔE) was 0.2−0.5 V, which is generally observed for aromatic hydrocarbons and other heterocyclic compounds. The second reduction and oxidation waves are irreversible, as is frequently observed for dications and dianions. The general instability of the dianions usually involves a subsequent homogeneous reaction that causes a shift of the waves to less extreme potentials (i.e., to more positive potentials for oxidation and more negative potentials for reduction).

Spectrometry. The same solvent used for electrochemical measurements was used for spectroscopic measurements. The absorption and fluorescence emission spectra of TphP, TnaP, and TpyP in MeCN:Bz (v:v = 1:1) solvent are shown in Figure 4. The results are summarized in Table 2. As these properties have already been investigated,[1] only a brief summary of the results is presented here for purposes of comparison to the electrochemical and ECL results. As observed from Figure 4, TphP shows two narrow absorption peaks at 278 and 329 nm (Figure 4a) and fluorescence with maxima at 375 and 393 nm (Figure 4d). The absorption is mainly located in the UV range and is due to the $\pi-\pi^*$ transition. Comparing the fluorescence spectra of these three phenanthrene derivatives, as the conjugation increases, a significant bathochromic shift is observed as the conjugation between the substituent group and phenanthrene core increases. These results are in agreement with the observed electrochemical data (as shown in Table 1) and results in ref 1 showing that the HOMO/LUMO energy gap of TpyP is substantially lower than those of
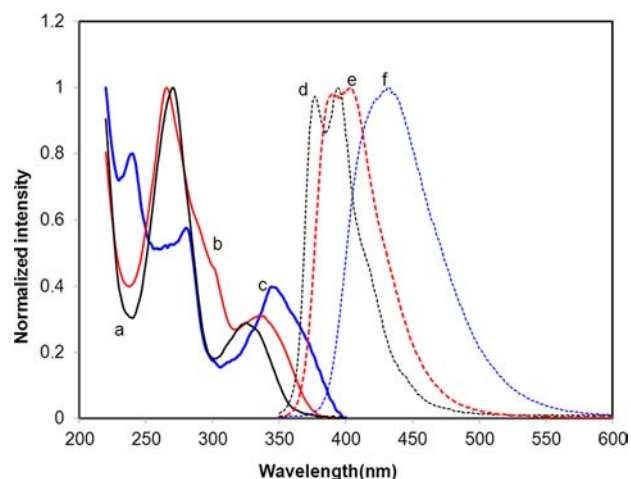

Figure 4. Normalized absorbance spectra (—) and fluorescence spectra (- - -) of phenanthrene compounds, TphP (black, a,d), TnaP (red, b,e), and TpyP (blue, c,f), in MeCN:Bz (v:v = 1:1). Emission spectra were excited at the absorption maximum.

TphP and TnaP due to the longer p-conjugation of the substituent group.

Electrogenerated Chemiluminescence (ECL). These three phenanthrene compounds are good candidates for ECL generation because of their high PL quantum yields and good electrochemical behavior. The physical and spectral data for the radical ion annihilation reaction for ECL were listed in Table 2. All compounds produced blue ECL emission that was visible to the naked eye in a dark room. The relative ECL quantum yields of these compounds were determined by comparing the number of photons emitted per electron with that for the standard ECL emitter, DPA. ECL efficiencies for the radical anion−cation annihilation are 0.004 for TphP, 0.16 for TnaP, and 0.25 for TpyP, respectively. The ECL efficiency increases with increases in the conjugation of the substituent groups appended to the phenanthrene, similarly to the electrochemical behavior.

Figure 5 shows the ECL spectra of the three phenanthrene compounds obtained by pulsing between 80 mV past the reduction peak potential and 80 mV past the oxidation peak potential with a pulse time of 0.1 s, respectively. The maximum ECL emissions of the three compounds were at the same position as those in fluorescence emissions (as shown in Supporting Information, Figures S11−S13). The difference in the ECL and the fluorescence spectrum can be ascribed to the different solutions and slit widths. Although ECL intensity was high (as shown in Supporting Information, Figure S14), little noisy signal was obtained because of the slit widths of 20 nm and quick ECL emission. The red shift observed in the ECL emission peaks proceeding from TphP, TnaP, and TpyP is consistent with the fluorescence spectra. The energy of the excited singlet state can be estimated from the fluorescence emission maximum by the equation E_s (eV) $= 1239.81/\lambda$ (nm), where λ is the wavelength at maximum emission. The calculated excited singlet state energies are listed in Table 2. The energies of the annihilation reaction, $-\Delta H° = E°_{ox} - E°_{red} - T\Delta S$, based on the difference between the thermodynamic potentials of the first oxidation and the first reduction in the cyclic energies ($E°_{ox} - E°_{red}$) with an estimated entropy effect (~0.1 eV) subtracted, are listed in Table 1. Table 2 shows that the energy of the annihilation reaction (3.66 eV for TphP, 3.52

Table 2. Photophysical Properties of the Three Studied Compounds in MeCN:Bz (v:v = 1:1)

	λ_{max} (abs) (nm)	ε (L mol^{-1} cm^{-1}) (10^3)	λ_{max} (fl) (nm)	Φfl^a	$E_s{}^b$	λ_{max} (ECL) (nm)	$\Phi_{ECL}{}^c$
TphP	278	8.40	375, 393	0.50	3.15	396	0.004
	329	3.02					
Tnap	265	28.37	389, 403	0.70	3.08	398	0.16
	338	8.1					
	240	11.22					
TpyP	280	8.7	427	0.87	2.90	437	0.25
	346	7.1					

^{a}DPA as the standard (Φ_{fl} = 0.88 in ethanol).[43] $^b E_s$: approximate energy of the singlet state taken as the fluorescence wavelength maximum, E_s = $1239.81/\lambda_{max}$ FL (nm). ^{c}ECL efficiencies are normalized with respect to DPA in MeCN (relative ECL efficiency of DPA is 1).
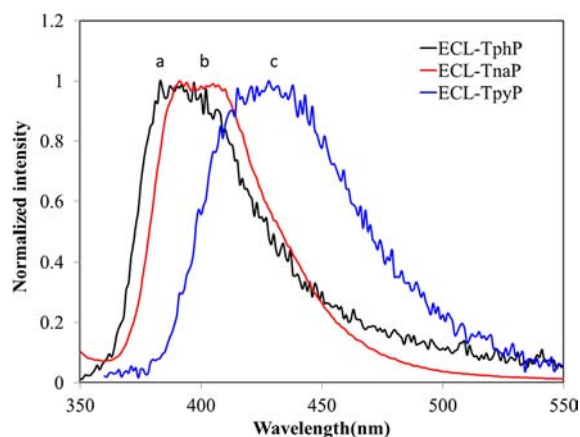

Figure 5. ECL spectra of TphP (black, a), TnaP (red, e,b), and TpyP (blue, c) generated through annihilation by pulsing the potential with a pulse width of 0.1 s from approximately 80 mV past the peaks potentials; slit width: 20 nm.
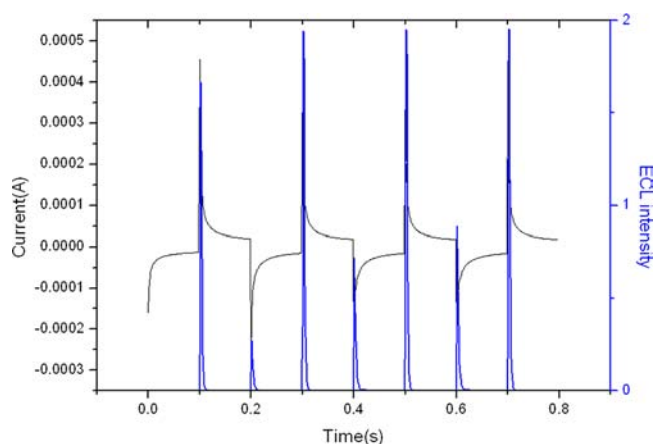

Figure 6. Initial current (black) and ECL light (blue) transients for 0.5 mM TphP pulsed between 80 mV past the first reduction peak and at 80 mV past the first oxidation potential, respectively. Pulse width is 0.1 s.

eV for TnaP, and 3.26 eV for TpyP) is greater than that needed to directly populate the singlet excited state (3.15 eV for TphP, 3.08 eV for TnaP, and 2.90 eV for TpyP); thus, the singlet excited states can be directly populated upon radical ion annihilation (S-route).

To estimate the stability of the ECL and the radical ion species, potential pulsing ECL transients were collected. When the radical ions are generated under mass-transfer controlled conditions and are stable during a pulse, the ECL emission pulses normally should be of equal height and constant with pulsing. However, when the potential was stepped from the reduction wave at E_{pc} − 80 mV to the oxidation wave at E_{pa} + 80 mV for the three compounds in this study, quick emission and different ECL intensities were observed for the cathodic and anodic pulses (as shown in Figure 6 and Supporting Information, Figure S15). For example, radical anion (TphP$^{-\bullet}$)−radical cation (TphP$^{+\bullet}$) annihilation produced by potential steps shows asymmetric ECL transients in which the cathodic pulse was always smaller than the anodic pulse (as shown in Figure 6). This behavior was independent of the direction of the first potential step. Essentially identical results for TnaP and TpyP are shown in Supporting Information, Figure S15.

This kind of ECL behavior suggests that the oxidized form is unstable and depleted in solution when the anodic pulse occurs. Only a fraction of the oxidized form is available for ECL, even though the current for its oxidation on a subsequent pulse is essentially the same. In previous work, we have shown through digital simulation that such behavior is expected when there are significant differences in the concentrations of the oxidizing and

reducing equivalents.[42] In this case, this behavior suggests that the instability of the cation results in a lower concentration of the cation radical, whereas the availability of a higher concentration of anion diffusing away from the annihilation zone and back during the following anodic pulse will lead to a larger emission and a more extended transient decay. Here, the difference in ECL intensities at different potential suggests the instability of the formed radical cations.

If one radical ion is too unstable, ECL can also be generated with a coreactant, such as BPO, which forms a strong oxidizing agent (+1.5 V vs SCE[43]) after being reduced. This strong oxidizing agent can react directly with the analyte anion and generate light without the radical cation. As shown in Figure 7a, a strong ECL signal visible to the naked eye in a lighted room was obtained upon the reduction of TphP in the presence of the coreactant BPO. Moreover, pulsing between 0 and −2.4 V vs Ag produced strong ECL emission. No ECL was obtained when the electrode potential was stepped back to 0.0 V, as expected. Under these conditions, we could also obtain an ECL spectrum, which exhibits a peak near that of ECL of TphP (Figure 7b). The same phenomena were observed for TnaP and TpyP (as shown in Supporting Information, Figure S16).

■ CONCLUSIONS

We have studied the electrochemistry and ECL behavior of three phenanthrene derivatives. These three derivatives show reversible reduction waves and less reversible oxidation waves at low scan rates. The oxidation waves of the CVs become more reversible, and the stability of radical cation increases as the conjugation of the substituent groups appended to the
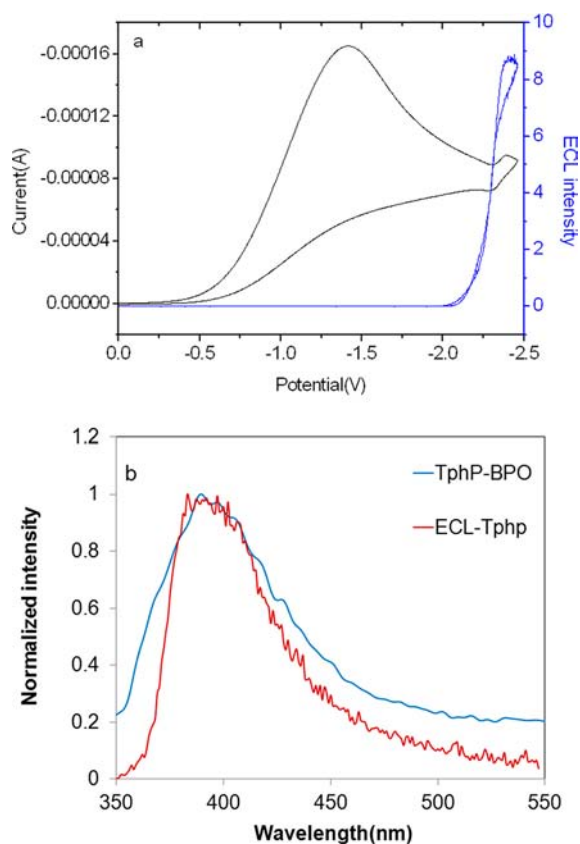
Figure 7. (a) ECL and CV simultaneous measurements for 0.5 mM TphP in the presence of 3.5 mM BPO; and (b) ECL spectra for 0.5 mM TphP in the absence (red) and presence (blue) of 3.5 mM BPO; spectra were generated by pulsing the potential from 0 to −2.4 V vs Ag in MeCN:Bz (v:v = 1:1) containing 0.1 M TBAPF$_6$.

phenanthrene increases. ECL was generated for all compounds by radical ion annihilation with an intensity that could be observed by the naked eye in a dark room and by a coreactant (BPO) with intensity visible to the naked eye in a lighted room. The ECL efficiency increases with the increased conjugation of the substituent groups appended to the phenanthrene. Transient ECL responses during anodic and cathodic pulses have unequal height due to the instability of the radical cation. This work demonstrates that the incorporation of different substituents into aromatic compounds can affect the luminescence efficiency and stability of radical ions, which will shape the future design of efficient ECL compounds for light-emitting displays.

ASSOCIATED CONTENT

Ⓢ Supporting Information

Simulated and experimental CVs, UV−vis spectra, fluorescence spectra, and ECL data. This material is available free of charge via the Internet at http://pubs.acs.org.

AUTHOR INFORMATION

Corresponding Author

ajbard@mail.utexas.edu

Notes

The authors declare no competing financial interest.

ACKNOWLEDGMENTS

REFERENCES

(1) Chen, Y. H.; Chou, H. H.; Su, T. H.; Chou, P. Y.; Wu, F. I.; Cheng, C. H. *Chem. Commun.* **2011**, *47*, 8865−8867.
(2) Miao, W. J. *Chem. Rev.* **2008**, *108*, 2506−2553.
(3) Choi, J. P.; Wong, K. T.; Chen, Y. M.; Yu, J. K.; Chou, P. T.; Bard, A. J. *J. Phys. Chem. B* **2003**, *107*, 14407−14413.
(4) Fungo, F.; Wong, K. T.; Ku, S. Y.; Hung, Y. Y.; Bard, A. J. *J. Phys. Chem. B* **2005**, *109*, 3984−3989.
(5) Rashidnadimi, S.; Hung, T. H.; Wong, K. T.; Bard, A. J. *J. Am. Chem. Soc.* **2008**, *130*, 634−639.
(6) Omer, K. M.; Kanibolotsky, A. L.; Skabara, P. J.; Perepichka, I. F.; Bard, A. J. *J. Phys. Chem. B* **2007**, *111*, 6612−6619.
(7) Shen, M.; Rodriguez-Lopez, J.; Lee, Y. T.; Chen, C. T.; Fan, F.-R. F.; Bard, A. J. *J. Phys. Chem. C* **2010**, *114*, 9772−9780.
(8) Omer, K. M.; Ku, S. Y.; Chen, Y. C.; Wong, K. T.; Bard, A. J. *J. Am. Chem. Soc.* **2010**, *132*, 10944−10952.
(9) Omer, K. M.; Ku, S. Y.; Cheng, J. Z.; Chou, S. H.; Wong, K. T.; Bard, A. J. *J. Am. Chem. Soc.* **2011**, *133*, 5492−5499.
(10) Maloy, J. T.; Bard, A. J. *J. Am. Chem. Soc.* **1971**, *93*, 5968−5981.
(11) Santhanam, K. S. V.; Bard, A. J. *J. Am. Chem. Soc.* **1965**, *87*, 139−140.
(12) Kesztheli, C. P.; Bard, A. J. *J. Org. Chem.* **1974**, *39*, 2936−2937.
(13) Keszthelyi, C. P.; Tokeltakvoryan, N. E.; Bard, A. J. *Anal. Chem.* **1975**, *47*, 249−256.
(14) Richards, T. C.; Bard, A. J. *Anal. Chem.* **1995**, *67*, 3140−3147.
(15) Sartin, M. M.; Shu, C. F.; Bard, A. J. *J. Am. Chem. Soc.* **2008**, *130*, 5354−5360.
(16) Suk, J.; Wu, Z. Y.; Wang, L.; Bard, A. J. *J. Am. Chem. Soc.* **2011**, *133*, 14675−14685.
(17) Lai, R. Y.; Bard, A. J. *J. Phys. Chem. B* **2003**, *107*, 5036−5042.
(18) Sartin, M. M.; Camerel, F.; Ziessel, R.; Bard, A. J. *J. Phys. Chem. C* **2008**, *112*, 10833−10841.
(19) Rosenthal, J.; Nepomnyashchii, A. B.; Kozhukh, J.; Bard, A. J.; Lippard, S. J. *J. Phys. Chem. C* **2011**, *115*, 17993−18001.
(20) Nepomnyashchii, A. B.; Broring, M.; Ahrens, J.; Kruger, R.; Bard, A. J. *J. Phys. Chem. C* **2010**, *114*, 14453−14460.
(21) Nepomnyashchii, A. B.; Cho, S.; Rossky, P. J.; Bard, A. J. *J. Am. Chem. Soc.* **2010**, *132*, 17550−17559.
(22) Suk, J.; Omer, K. M.; Bura, T.; Ziessel, R.; Bard, A. J. *J. Phys. Chem. C* **2011**, *115*, 15361−15368.
(23) Lee, S. K.; Zu, Y. B.; Herrmann, A.; Geerts, Y.; Mullen, K.; Bard, A. J. *J. Am. Chem. Soc.* **1999**, *121*, 3513−3520.
(24) Lai, R. Y.; Fleming, J. J.; Merner, B. L.; Vermeij, R. J.; Bodwell, G. J.; Bard, A. J. *J. Phys. Chem. A* **2004**, *108*, 376−383.
(25) Sartin, M. M.; Boydston, A. J.; Pagenkopf, B. L.; Bard, A. J. *J. Am. Chem. Soc.* **2006**, *128*, 10163−10170.
(26) Lai, R. Y.; Fabrizio, E. F.; Lu, L. D.; Jenekhe, S. A.; Bard, A. J. *J. Am. Chem. Soc.* **2001**, *123*, 9112−9118.
(27) Lai, R. Y.; Kong, X. X.; Jenekhe, S. A.; Bard, A. J. *J. Am. Chem. Soc.* **2003**, *125*, 12631−12639.
(28) Ho, T. I.; Elangovan, A.; Hsu, H. Y.; Yang, S. W. *J. Phys. Chem. B* **2005**, *109*, 8626−8633.
(29) Oh, J. W.; Lee, Y. O.; Kim, T. H.; Ko, K. C.; Lee, J. Y.; Kim, H.; Kim, J. S. *Angew. Chem., Int. Ed.* **2009**, *48*, 2522−2524.
(30) Jiang, X.; Yang, X. C.; Zhao, C. Z.; Jin, K.; Sun, L. C. *J. Phys. Chem. C* **2007**, *111*, 9595−9602.

(31) Hallas, G.; Hepworth, J. D.; Waring, D. R. *J. Chem. Soc. B* **1970**, 975−979.

(32) Boden, B. N.; Jardine, K. J.; Leung, A. C. W.; MacLachlan, M. J. *Org. Lett.* **2006**, *8*, 1855−1858.

(33) Grisorio, R.; Suranna, G. P.; Mastrorilli, P.; Nobile, C. F. *Org. Lett.* **2007**, *9*, 3149−3152.

(34) Song, S.; Jin, Y.; Kim, K.; Kim, S. H.; Shim, Y. B.; Lee, K.; Suh, H. *Tetrahedron Lett.* **2008**, *49*, 3582−3587.

(35) He, B.; Tian, H. K.; Geng, Y. H.; Wang, F. S.; Mullen, K. *Org. Lett.* **2008**, *10*, 773−776.

(36) Tian, H. K.; Shi, J. W.; Dong, S. Q.; Yan, D. H.; Wang, L. X.; Geng, Y. H.; Wang, F. S. *Chem. Commun.* **2006**, 3498−3500.

(37) Yang, C.; Jacob, J.; Mullen, K. *Macromolecules* **2006**, *39*, 5696−5704.

(38) Yang, C. D.; Scheiber, H.; List, E. J. W.; Jacob, J.; Mullen, K. *Macromolecules* **2006**, *39*, 5213−5221.

(39) Sahami, S.; Weaver, M. J. *J. Electroanal. Chem.* **1981**, *122*, 155−170.

(40) Yang, H. G.; Bard, A. J. *J. Electroanal. Chem.* **1991**, *306*, 87−109.

(41) Denuault, G.; Mirkin, M. V.; Bard, A. J. *J. Electroanal. Chem.* **1991**, *308*, 27−38.

(42) Shen, M.; Rodriguez-Lopez, J.; Huang, J.; Liu, Q. A.; Zhu, X. H.; Bard, A. J. *J. Am. Chem. Soc.* **2010**, *132*, 13453−13461.

(43) Chandros, E. A.; Sonntag, I. *J. Am. Chem. Soc.* **1966**, *88*, 1089−1096.